World Academy of Science, Engineering and Technology
International Journal of Civil and Environmental Engineering
Vol:7, No:6, 2013

Sub-Impact Phenomenon of Elasto-Plastic Free-Free Beam during a Strike

H. Rong, X. C. Yin, J. Yang, and Y. N. Shen

***Abstract*—**Based on Rayleigh beam theory, the sub-impacts of a free-free beam struck horizontally by a round-nosed rigid mass is simulated by the finite difference method and the impact-separation conditions. In order to obtain the sub-impact force, a uniaxial compression elastic-plastic contact model is employed to analyze the local deformation field on contact zone. It is found that the horizontal impact is a complicated process including the elastic plastic sub-impacts in sequence. There are two sub-zones of sub-impact. In addition, it found that the elastic energy of the free-free beam is more suitable for the Poisson collision hypothesis to explain compression and recovery processes.

***Keywords*—**beam, sub-impact, elastic-plastic deformation, finite difference method.

I. Introduction

THE impact problem of free slender flight objects, such as rockets and missiles struck by projectiles, has attracted international attention [1], [2]. The slender free flight objects are usually modeled as free-free beams to simulate impact dynamic behaviors.

The sub-impact phenomenon has been observed in some numerical and experimental researches for restrained flexible beams [3]-[5]. In the experiment and simulation of a falling beam on the fixed ground, Stoianovici and Hurmuzlu [6] captured 19 times of sub-impact by means of high-speed photoelectric measurement, and Shann et al. [7] found the subsequent sub-impacts might be larger than initial ones due to different angles of impact by the three-dimensional simulation modeling.

For a free-free beam struck by a flight body, Yang and Xi [8] have obtained the photographs of local contact deformation and final bending folded flying attitude by a high speed camera system. Yang and Yin et al. [9], [10] simulated the phenomena of plastic sub-impact and elastic viscoplastic sub-impact by the theories of rigid-plastic dynamics and MEVP method, respectively. The present study focuses on the phenomenon of elasto-plastic sub-impacts of two free flight bodies, i.e., a free-free beam struck by a round-nosed rigid mass, by the theory of elasto-plasticity.

H. Rong is with the Mechanics Department of Nanjing University of Science and Technology, Nanjing, Jiangsu 210094 China (phone: 86-13951854280; e-mail: rh426@139.com).

X. C. Yin is with the Mechanics Department of Nanjing University of Science and Technology, Nanjing, Jiangsu 210094 China (e-mail: yinxiaochun2000@yahoo.com.cn).

J. Yang is with the New United Group Co., Ltd., Changzhou, Jiangsu 213000 China.

Y. N. Shen is with the Mechanics Department of Nanjing University of Science and Technology, Nanjing, Jiangsu 210094 China.

II. The Impact System and Solving Method

A. Impact System Model

Fig. 1 shows an impact system, a free-free beam horizontally struck at the middle by a round-nosed rigid mass. The beam is of length l, thickness h, width b, volume density ρ, Young's modulus E, and yield stress Y. The rigid mass is of mass m, nose radius R, and initial impact velocity v_0. The beam is molded as the Rayleigh beam. A linear elastic-perfectly plastic constitutive relation is adopted and small displacements are assumed, i.e., geometrical nonlinearity is neglected. The choose of horizontal impact is to avoid the mass bounce caused by gravitational potential energy disturbing the observation of sub-impact phenomena.

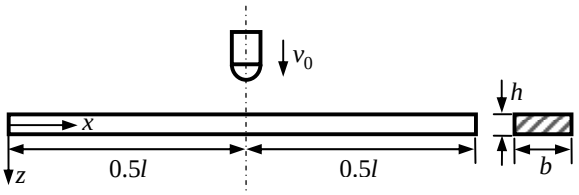

Fig. 1 Structure model

B. Equations of Motion

Based on the Rayleigh beam theory, the equation of the motion of the free-free beam is

$$\frac{\partial^2 M}{\partial x^2} + J\frac{\partial^4 w}{\partial x^2 \partial t^2} + q(x,t) = \rho A\frac{\partial^2 w}{\partial t^2} \tag{1}$$

where t is the time, w the transverse displacement, M the bending moment of a cross-section, J the rotary inertia of a cross-section per unit length, A the cross section area, $q(x,t)$ the line distribution external load. $q(x,t)$ is the distribution impact pressure per unit length resulted from the impact force $F(t)$.

The round-nosed rigid mass moves in deceleration under the impact force, and moves in uniform velocity during the separation from the free-free beam. Its equation of motion is

$$-m\ddot{w}_M = \begin{cases} F(t) & impact \\ 0 & seperation \end{cases} \quad (2)$$

where w_M is the displacement, and $\ddot{w}_M$ the acceleration.

C. Elastic Plastic Contact Model

Ignoring the deformation of the rigid mass, only the local contact deformation resulted by rigid indentation of the round-nosed rigid mass on the surface of the beam. The local contact deformation is calculated by the generalized elastic plastic foundation model [11] (Fig. 2). The model should be modified to be suitable for the local elasto-plastic deformation of sub-impacts.

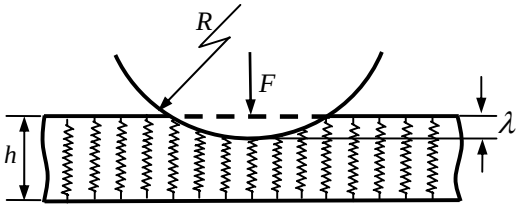

Fig. 2 Uniaxial compression elastic-plastic contact model

During the first sub-impact, the rigid indentation can be divided into the three stages. The first stage is elastic indentation. Then plastic indentation might be taken place. The final stage is elastic unloading. If sub-impact takes place more than one time, and the local plastic contact deformation has already formed before, the cumulate residual plastic indentation should be taken into account.

Generally, during the n-th impact, the contact between the round-nosed rigid mass and the beam takes place only when the indentation λ exceeds the residual plastic indentation λ_r^{n-1} of the $(n-1)$-th impact, and generates new impact force. Condition of new plastic indentation during the n-th impact is that λ is larger than the maximum indentation λ_m^{n-1} before. Hence, the general relationship between the impact force F_n in the n-th impact and the indentation λ can be derived as follows:

(a) in the elastic indentation stage,

$$F_1 = \frac{4\sqrt{2R}Eb}{3h}\lambda^{3/2},\ \lambda \le \lambda_s$$
$$F_n = \frac{4\sqrt{2R}Eb}{3h}\left[\lambda^{3/2} - \left(\lambda_m^{n-1} - \lambda_s\right)^{3/2}\right]$$
$$\lambda \le \lambda_m^{n-1}\ ,\ \mathrm{n}>1 \quad (3)$$

(b) in the plastic indentation stage,

$$F_n = \frac{4\sqrt{2R}Eb}{3h}\left[\lambda^{3/2} - \left(\lambda - \lambda_s\right)^{3/2}\right]$$
$$\lambda > \lambda_s (n=1),\ \ \lambda > \lambda_m^{n-1}(n>1) \quad (4)$$

(c) in the elastic unloading stage,

$$F_1 = \frac{4\sqrt{2R}Eb}{3h}\left[\lambda^{3/2} - \left(\lambda_m^1 - \lambda_s\right)^{3/2}\right]$$
$$F_n = \frac{4\sqrt{2R}Eb}{3h}\left[\lambda^{3/2} - \left(\lambda_m^{n-1} - \lambda_s\right)^{3/2}\right]$$
$\lambda_m^n \le \lambda_m^{n-1}(n>1)$, after unloading, make $\lambda_m^n = \lambda_m^{n-1}$
$$F_n = \frac{4\sqrt{2R}Eb}{3h}\left[\lambda^{3/2} - \left(\lambda_m^n - \lambda_s\right)^{3/2}\right]$$
$$\lambda_m^n > \lambda_m^{n-1}(n>1) \quad (5)$$

where the residual indentation is

$$\lambda_r^n = \lambda_m^n - \lambda_s \quad (6)$$

The indentation and the impact force are both functions that change with time.

D. Impact-Separation Conditions

The impact condition is determined by displacement and the separation condition by impact force, respectively, in order to avoid the contact tensile stress when both the conditions are determined by displacement [12]. The unified impact - separation conditions are given by

$$F_n \cdot (w_m - w(0.5l) - \delta_r^{n-1}) = 0 \quad (7)$$

where w_m is the displacement of the round-nosed rigid mass, $w(0.5l)$ is the displacement of the middle of the beam.

E. Solving Method

As shown in Fig. 3, the beam is divided into $(2k+1)$ equidistant micro segments in the axial direction, and $2p$ ones in the height direction.

Generally, the local contact area caused by impact is quite narrow, so that the impact force can be applied to the $(k+1)$th segment as a concentrated force.

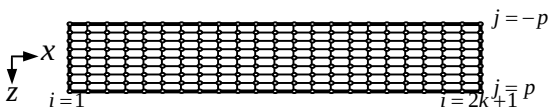

Fig. 3 Discrete model of free-free beam

The equation of motion of the beam can be discretized by central difference formula. On the $(k+1)$th segment where the impact force acts, the discrete equation of motion is

$$M_{k+2} - 2M_{k+1} + M_k + \rho' J\left(\ddot{w}_{k+2} - 2\ddot{w}_{k+1} + \ddot{w}_k\right) + F\Delta x = \rho' A\ddot{w}_{k+1}(\Delta x)^2 \quad (8)$$

According to the boundary conditions, the discrete equations of motion of the left and right boundary of the beam are given respectively as follows:

$$M_1 - M_0 + \rho J\left(\ddot{w}_1 - \ddot{w}_0\right) = \rho A \ddot{w}_0 \left(\Delta x\right)^2 \quad (9)$$

$$M_{2k} - M_{2k+1} + \rho J\left(\ddot{w}_{2k} - \ddot{w}_{2k+1}\right) = \rho A \ddot{w}_{2k+1} \left(\Delta x\right)^2 \quad (10)$$

The discrete equation of motion of the other segments is

$$M_{i+1} - 2M_i + M_{i-1} + \rho J\left(\ddot{w}_{i+1} - 2\ddot{w}_i + \ddot{w}_{i-1}\right) = \rho A \ddot{w}_i (\Delta x)^2$$
$$(i = 2, \ldots, k, k+2, \ldots, 2k) \quad (11)$$

The beam constitutive relations in the incremental form can be given by

$$\sigma = \begin{cases} E\varepsilon, & |\varepsilon| \le \varepsilon_s \\ Y sign\varepsilon, & |\varepsilon| > \varepsilon_s, \sigma d\varepsilon > 0 \\ \sigma^* + d\sigma, d\sigma = E d\varepsilon, & |\varepsilon| \le \varepsilon_s, \sigma d\varepsilon < 0 \end{cases} \quad (12)$$

where ε is the strain, σ is the stress, σ^* is the stress of the previous instant.

The described solving method, so called MCIS method [11], was first presented for the multiple impact problems. It's applied to the present sub-impact problem according to the hypothesis that the contact wave effect along the beam thick during the sub-impact can be negligible.

III. The Example and Analyses

The sizes of the round-nosed rigid mass and the free-free beam are R=0.01m, l=0.7112m, b=0.0163m, and h=0.0075m. The round-nosed rigid mass has m=0.201kg and v_0=15.9m/s, the beam material parameters are ρ=2600kg/m^3, E=71.96GPa, and Y=150MPa. The beam is made of aluminum alloy and is not sensitive to the rate of strain. The free-free beam is discretized into 501 segments in the axial direction, and 40 layers in the height direction. The solving time step is 0.1μs.

A. Phenomena of Elasto-Plastic Sub-Impacts

Fig. 4 shows the impact force F, the displacement of the middle of the beam (impact end) $w_c = w(0.5l)$, the displacement of the round-nosed rigid mass w_m, within the entire process of the strike of the round-nosed rigid mass on the free-free beam. The deformation of the impact end of the beam f_c is shown as well in Fig. 4. f_c is calculated as the relative displacement between the impact end and the free end, $f_c = w_c - w(x=0)$. The entire strike lasts for 7.031ms, which looks like an impact by the naked eyes. But it contains indeed 57 times of sub-impacts. The first sub-impact lasts for 203 microseconds, and others last for about several tens of microseconds.

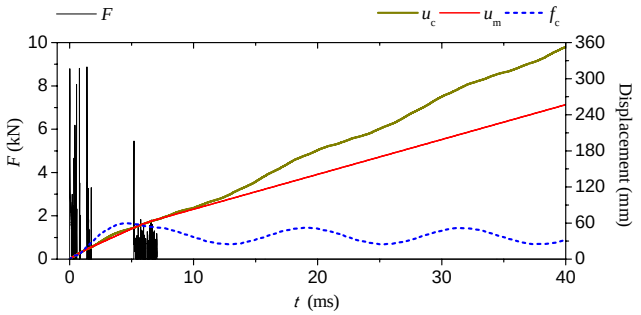

Fig. 4 Response of impact force and displacement

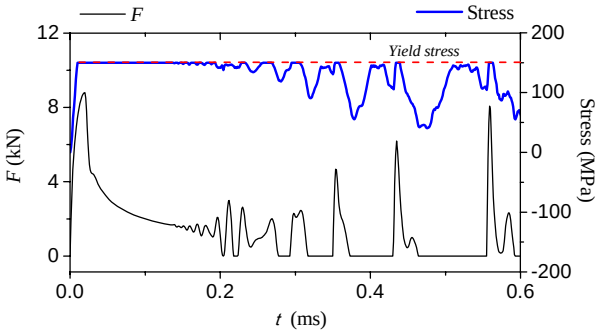

Fig. 5 Response of impact force and stress

In the first sub-impact, plastic deformation has taken place as shown in Fig. 5, where the blue line of the beam stress responses at the back surface of the contact point has reached at 9.9 microsecond the yield stress Y=150MPa. In the subsequent sub-impacts the stress can also reach the yield stress.

In Fig. 6, the contact plastic deformation in the first sub-impact firstly takes place in the marked point A on the curve of the impact force vs. indentation. The marked point B is the beginning of unloading in the first sub-impact. The indentation of point B is 0.169mm, while the indentation of point A is 0.015mm. During the entire strike, there are other plastic indentations in some sub-impacts, for example, as shown in the small plots in Fig. 6.

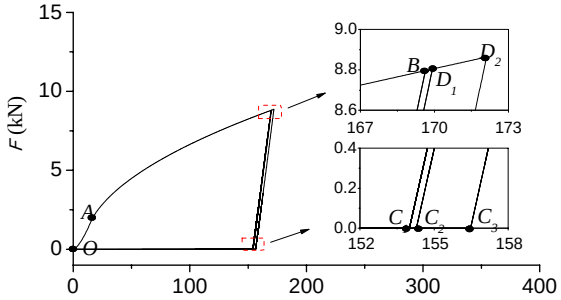

Fig. 6 Variation of impact force and indentation

The results of Fig. 5 and Fig. 6 illustrate that the phenomena of sub-impact observed in Fig. 4 is the phenomena of elasto-plastic sub-impact.

B. Partition of Impact

Interestingly, it is found that the sub-impacts take place intensively in two impact zones, such partition phenomenon of sub-impacts was first observed by Yin [13]. The first impact zone lies in 0-1.757ms, which contains 18 times of impacts. The second one lies in 5.178-7.031ms, which contains 39 times of impacts. Between the two impact zones, there is a separation zone of 3.42ms. In addition, there are two sub-zones observed in the first impact zone.

C. The Compression Zone and Recovery Zone of Impact

The moving state of the free-free beam is much different from that of a restrained beam when struck. In Fig. 4, unlike a restrained beam, it can be seen that the free-free beam moves ahead along the impact direction all the time. However, the deformation state in Fig. 7 in the expression of f_c and u_{mf} is similar to that of a restrained beam [14], where u_{mf} is the relative displacement between the round-nosed rigid mass and the free end of the free-free beam.

When a restrained beam is struck by a rigid mass, the rigid mass rebounds finally and obtains a rebound velocity. The rebound kinetic energy comes from the release of the energy of the beam. While as shown in Fig. 7, the kinetic energy U_m of the round-nosed rigid mass loses continuously until the end of the strike. It obtains no energy from the free-free beam. There is no recovery process defined by the Poisson collision hypothesis that can release the energy from the free-free beam to rebound the round-nosed rigid mass.

However, the elastic energy U_e of the free-free beam increases overall in the first impact zone and separation zone, and decreases in the second impact zone. It means that there is the elastic energy releasing of the free-free beam in the second impact zone. The releasing elastic energy is absorbed not by the round-nosed rigid mass but by the free-free beam itself. It transfers into the kinetic energy U_k and plastic energy of the free-free beam.

In the first impact zone, the elastic energy U_e undergoes increasing and decreasing processes as well. It increases in the first sub-zone and decreases overall in the second sub-zone and separation sub-zone.

Therefore, although there is no recovery process defined by the Poisson collision hypothesis, from the perspective of the rebound velocity or the rebound energy of the round-nosed rigid mass, but there is the compression and recovery process in view of the elastic energy of the free-free beam.

The present study gives that the elastic energy is suitable for the Poisson collision hypothesis to explain compression and recovery processes, for which the kinetic energy of impacted and impacting body is not suitable.

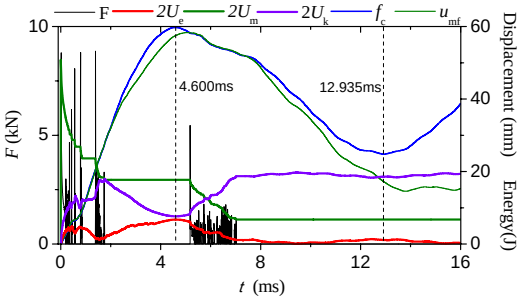

Fig.7 Response of impact force and relative displacement

REFERENCES

[1] Jones N, Wierzbicki T. "Dynamic plastic failure of a free-free beam." International Journal of Impact Engineering, 1987, 6(3): 225-240.

[2] Q. Zhang, X. Wang, F. Huang, et al. "An experimental and numerical study of the dynamic response of a free-free aluminum beam under high velocity transverse impact." International Journal of Impact Engineering, 2009, 36(12): 1385-1393.

[3] X.C. Yin, Y. Qin, H. Zou, 2007. "Transient responses of repeated impact of a beam against a stop," Int. J. Solids Struct, 44(22-23): 7323–7339.

[4] Z.H. Liu, X.C. Yin, 2010. "Multiple elastic-plastic impacts of a variable cross-section beam struck by a round-nosed rigid mass in an impact course." Engineering Mechanics, 27(11): 244-249. (in Chinese)

[5] Melcher J , Xu X, Ramana A, 2008. "Multiple impact regimes in liquid environment dynamic atomic force microscopy," Appl. Phys. Lett., 93(9): 093111.

[6] Stoianovici D, Hurmuzlu Y, 1996. "A critical study of the applicability of rigid-body collision theory," ASME J. Appl. Mech., 63(2): 307–316.

[7] H. Shan, J.H. Su, Zhu J S, Xu L, 2007. "Three-dimensional modeling and simulation of a falling electronic device," ASME J. Comput. Nonlinear Dynam., 2(1): 22-31.

[8] J.L. Yang, F. Xi. "Experimental and theoretical study of free-free beam subjected to impact at any cross-section along its span. " International Journal of Impact Engineering, 2003, 28(7): 761-781.

[9] J. Yang, X.C. Yin, Z.H. Liu, P.B. Qian. "Sub-plastic impacts of rigid mass on free-free beam." Journal of Nanjing University of Science and Technology , 2012, 35(6) : 837-842.

[10] J. Yang, X.C. Yin, Z.H. Liu, P.B. Qian. "Elastic viscoplastic sub-impacts of free-free beam struck by rigid mass." Journal of Mechanical Engineering, 2012, 48(1) : 72~77.

[11] Z.H. Liu, X.C. Yin. "Multiple elastic-plastic impacts between free-free beam and simply supported beam." Journal of Mechanical Engineering, 2010, 46(10): 47-53.

[12] Z.F. Nie, G.T. Yang. "Experimental investigation on large deflection response of a frame impacted by a moving body." Acta Mechanica Solida Sinica, 1991, 12(1): 44-54.

[13] X.C. Yin. "Multiple impacts of two concentric hollow cylinders with zero clearance. International Journal of Solids and Structures," 1997. 34(35-36): 4597-4616.

[14] Z.H. Liu, X.C. Yin. "Multiple elastic-plastic impacts of a simply supported beam struck by a round-nosed mass." Explosion and Shock Waves, 2010, 30(2): 138-144.